OPEN

Citation: Transl Psychiatry (2017) 7, e1185; doi:10.1038/tp.2017.149

www.nature.com/tp

ORIGINAL ARTICLE

A novel preventive therapy for paclitaxel-induced cognitive deficits: preclinical evidence from C57BL/6 mice

P Huehnchen[1,2,3,8], W Boehmerle[1,2,3,8], A Springer[4], D Freyer[1,5] and M Endres[1,2,3,5,6,7]

Chemotherapy-induced central nervous system (CNS) neurotoxicity presents an unmet medical need. Patients often report a cognitive decline in temporal correlation to chemotherapy, particularly for hippocampus-dependent verbal and visuo-spatial abilities. We treated adult C57Bl/6 mice with 12×20 mg kg^{-1} paclitaxel (PTX), mimicking clinical conditions of dose-dense chemotherapy, followed by a pulse of bromodesoxyuridine (BrdU) to label dividing cells. In this model, mice developed visuo-spatial memory impairments, and we measured peak PTX concentrations in the hippocampus of 230 nM l^{-1}, which was sevenfold higher compared with the neocortex. Histologic analysis revealed a reduced hippocampal cell proliferation. *In vitro*, we observed severe toxicity in slowly proliferating neural stem cells (NSC) as well as human neuronal progenitor cells after 2 h exposure to low nanomolar concentrations of PTX. In comparison, mature post-mitotic hippocampal neurons and cell lines of malignant cells were less vulnerable. In PTX-treated NSC, we observed an increase of intracellular calcium levels, as well as an increased activity of calpain- and caspase 3/7, suggesting a calcium-dependent mechanism. This cell death pathway could be specifically inhibited with lithium, but not glycogen synthase kinase 3 inhibitors, which protected NSC *in vitro*. *In vivo*, preemptive treatment of mice with lithium prevented PTX-induced memory deficits and abnormal adult hippocampal neurogenesis. In summary, we identified a molecular pathomechanism, which invokes PTX-induced cytotoxicity in NSC independent of cell cycle status. This pathway could be pharmacologically inhibited with lithium without impairing paclitaxel's tubulin-dependent cytostatic mode of action, enabling a potential translational clinical approach.

Translational Psychiatry (2017) **7,** e1185; doi:10.1038/tp.2017.149; published online 1 August 2017

INTRODUCTION

Neurotoxic phenomena are common adverse effects of antineoplastic chemotherapy. In the peripheral nervous system, the development of chemotherapy-induced peripheral neuropathy is a well-recognized adverse reaction for many substances (reviewed by ref. 1). Side effects of chemotherapy in the central nervous system (CNS), in particular, changes in cognitive function (in the non-medical literature often referred to as 'chemobrain' or 'chemofog'), are more diffuse. A growing body of evidence underlines the potential of cytostatic drugs to induce cognitive deficits in humans (reviewed by ref. 2); however, many questions regarding which substances are capable of inducing this effect as well as the underlying molecular mechanisms remain unclear. Patients suffering from post-chemotherapy cognitive impairments (PCCI) typically report a decline in verbal and visuo-spatial abilities, executive functions, processing speed and attention span. Meta-analyses from clinical studies show that patients receiving chemotherapy performed significantly worse in standardized neuropsychological tests, mainly in the verbal and visuo-spatial domains.[3,4] A number of putative pathomechanisms underlying PCCI were proposed and include among others (1) mutations in p-glycoprotein and apolipoprotein E e4, (2) hormonal changes with reduction of neuroprotective estrogen, (3) DNA damage due to oxidative stress, (4) chronic ischemia related to anemia and coagulopathies, (5) dysregulation of the immune system with an increase of pro-inflammatory cytokines and (6) a reduction of adult hippocampal neurogenesis (reviewed by ref. 5). Considering the clinical symptoms as well as radiological findings,[6] an impaired adult hippocampal neurogenesis due to chemotherapy-induced toxicity presents an intriguing hypothesis.

Another interesting phenomenon is that PCCI also seems to occur in patients who received chemotherapeutics with poor blood–brain barrier (BBB) penetration.[7,8] Paclitaxel (PTX) is a microtubule-stabilizing agent that is frequently used to treat a wide spectrum of solid tumors such as breast, ovarian and non-small cell lung cancer (reviewed by ref. 9). It is a highly lipophilic substance that easily crosses the BBB, however it is quickly eliminated from the CNS by an active (p-glycoprotein-mediated) transporter mechanism.[10] Despite poor BBB penetration PTX-induced transient encephalopathy is well documented.[11–13] Although PCCI was reported in patients with PTX combination therapy (for example, ref. 14), the question whether PTX treatment

[1]Charité – Universitätsmedizin Berlin, Corporate Member of Freie Universität Berlin, Humboldt-Universität zu Berlin, and Berlin Institute of Health, Klinik und Hochschulambulanz für Neurologie, Berlin, Germany; [2]Charité – Universitätsmedizin Berlin, Corporate Member of Freie Universität Berlin, Humboldt-Universität zu Berlin, and Berlin Institute of Health, Neurocure Cluster of Excellence, Berlin, Germany; [3]Berlin Institute of Health (BIH), Berlin, Germany; [4]Großgerätezentrum BioSupraMol, Department of Biology, Chemistry and Pharmacy, Institute of Chemistry and Biochemistry, Freie Universität Berlin, Berlin, Germany; [5]Charité – Universitätsmedizin Berlin, Corporate Member of Freie Universität Berlin, Humboldt-Universität zu Berlin, and Berlin Institute of Health, Center for Stroke Research Berlin, Berlin, Germany; [6]German Centre for Neurodegenerative Diseases (DZNE), Berlin, Germany and [7]DZHK (German Centre for Cardiovascular Research), partner site Berlin, Berlin, Germany. Correspondence: Dr W Boehmerle, Klinik und Hochschulambulanz für Neurologie, Charité Universitätsmedizin Berlin, Chariteplatz 1, Berlin 10117, Germany.
E-mail: wolfgang.boehmerle@charite.de
[8]These authors contributed equally to this work.
Received 2 January 2017; revised 18 May 2017; accepted 7 June 2017

can induce memory deficits in rodents remains controversial with some studies reporting an effect of taxanes (PTX or docetaxel) on rodent cognition,[15–17] while others do not.[18]

In the present study, we aimed to characterize the effects of dose-dense PTX therapy, a clinical treatment regimen that uses smaller dosages in more frequent applications,[19] on spatial learning and memory in C57Bl/6 mice. More importantly, we aimed to further elucidate the cellular and molecular mechanisms of cytotoxicity and to establish a preventive strategy.

MATERIALS AND METHODS

Experimental procedures are described in more detail in the Supplementary Information.

In vitro

Cell culture. All experimental procedures conformed to institutional guidelines and were approved by an official committee (Landesamt für Gesundheit und Soziales, Berlin, Germany). Microdissection, preparation and maintenance of mouse neural stem cells (NSC) on 2- to 4-week-old C57Bl/6 mice were conducted as described previously.[20] The ability of cells to generate neurons and glia were routinely checked. For cytotoxicity and caspase assays, cells were plated on 96-well flat bottom plates (BD Biosciences, Billerica, MA, USA) and PTX toxicity was induced 24 h after passage of cells. Preparation and culture of hippocampal neurons (HCN) was conducted on C57Bl/6 embryos E14 as published previously.[21] Human neuronal progenitor cells were derived from human pluripotent stem cells by dual SMAD inhibition as described before.[22] Cell differentiation was confirmed by staining for Nestin, SOX 1 and 2 as well as PAX-6 (A24354, ThermoFisher, Darmstadt, Germany) prior to toxicity analysis. For cytotoxicity and caspase assays, cells were plated on 96-well flat bottom plates (BD Biosciences) and cytotoxicity experiments were conducted with the same protocol as for NSC. MCF-7 and HeLa cell lines were obtained from Sigma-Aldrich (Taufkirchen, Germany; Authentication by STR profiling). Cell culture was performed as described before.[23]

Live cell imaging. Imaging of NSC cultured on 8 well Ibidi µ-Slides (Ibidi, Martinsried, Germany) and loaded with 5 µM Fura-2/AM was performed as described previously.[24] Resting Ca^{2+} concentrations were measured after incubation for 2 h with 30 nM PTX or vehicle (VEH).

Cell viability and caspase activity assays. Cell viability was calculated as a compound measure of cytotoxicity and metabolic integrity and caspase activity was measured with commercial assays as described previously.[24]

Fluorescent-activated cell sorting. DNA content was determined by staining with propidium iodide (Abcam, Cambridge, UK) after exposure of NSC with PTX or VEH. Cells were measured immediately on a FACS Canto II (BD Biosciences, Heidelberg, Germany). Data were obtained from three individual experiments and analyzed using FlowJo software (Ashland, OR, USA).

Western blot analysis. Lysate preparation and immunoblotting was performed with as reported previously.[25]

In vivo

Animal numbers, housing conditions and study approval. A total of 127 nine-week old male C57BL/6 N mice from Charles River (Sulzfeld, Germany) were used for this study. All experimental procedures conformed to animal welfare guidelines and were previously approved by an official committee (Landesamt für Gesundheit und Soziales, Berlin, Germany). Mice were housed in groups of five in an enriched environment and allowed food and water *ad libitum*. The animals were maintained on a 12:12 h light/dark cycle (0700 hours–1900 hours) and behavioral testing was conducted between 1000 hours and 1600 hours. Injections coinciding with behavior tests were administered after all testing had been completed. The general wellbeing of the mice was assessed daily and their weight recorded on a regular basis.

Sample sizes and methods of randomization and blinding. We chose a mouse model of dose-dense PTX therapy to evaluate changes of cognition induced by PTX treatment.[26] Overall four different sets of animal experiments were performed: (1) In the initial trial, we used 15 animals for the treatment and 10 animals for the control group, as previous studies reported a mortality of 25–50% for repeated 20 mg kg^{-1} body weight (BW) PTX injections in mice.[27] (2) In the second experiment, we studied possible traits of anxiety and depression. We determined the group size based on the observations of the first experiment, with a desired power of 0.8 and an alpha level of 0.05 using SigmaPlot software (Systat, Richmond, CA, USA). Having expected a smaller effect size, we calculated $n = 15$ animals per group. (3) An additional 12 PTX and lithium carbonate (Li^+)-injected animals were used to measure pharmacokinetics (2 mice per time point as described below). (4) In the last step, a preventive application of Li^+ in PTX and VEH-treated mice was assessed. The calculated sample size with four different groups (VEH/VEH; PTX/VEH; VEH/Li^+; PTX/Li^+) was $n = 15$ animals per group.

Upon arrival of the animals in the animal facility, unequal block randomization was performed[28] to determine group and cage allocation. All injections of substances (PTX; VEH; Li^+) were carried out by one examiner. The investigators conducting the behavior experiments as well as histological analysis were blinded throughout the entire process including statistical analysis.

Drug injection protocol. PTX (Sigma-Aldrich) was dissolved in Cremophor EL: Ethanol (1:1) to a concentration of 6 mg ml^{-1} and diluted in sterile 0.9% NaCl solution to a final concentration of 2 mg ml^{-1} before intraperitoneal (i.p.) injection of 20 mg kg^{-1} BW PTX. Animals in the control group received an equal volume of vehicle (Cremophor EL: Ethanol, 1:1, diluted in sterile 0.9% NaCl solution to a final concentration of 33.3% Cremophor EL: Ethanol) via i.p. injection.

For the interventional trial, lithium carbonate (Li^+) was dissolved in sterile 0.9% NaCl solution to a final concentration of 1.28 mg ml^{-1} before i.p. injection and 170 µM Li^+/kg BW were injected before administration of PTX or VEH.

5-Bromo-2′-deoxyuridine (BrdU; Sigma-Aldrich) was dissolved in 0.9% sterile NaCl and injected at a concentration of 50 mg kg^{-1} i.p. 24 h after the last PTX injection to label dividing cells in all experiments.

Pharmacokinetic analysis. After injection of 20 mg kg^{-1} PTX, respectively, 170 µM Li^+, two animals each were maintained for 15, 30, 60, 120, 240 and 720 min before final anesthesia. Blood was drawn from the V. cava inferior before exsanguination with 0.9% NaCl. Brains were rapidly extracted, dissected and snap frozen in liquid nitrogen. Blood samples were centrifuged and remaining serum was snap frozen in liquid nitrogen. Samples were prepared for analysis with liquid chromatography-tandem mass spectrometry with an adapted previously described protocol.[29] Analysis was performed by UPLC-MS/MS with an Acquity UPLC—Synapt G2-S HDMS system equipped with an Acquity UPLC C18 1.7 µm 2.1 × 50 mm column (all by Waters, Eschborn, Germany). For MS/MS experiments, the $[M+H]^+$ ion with *m/z* 854.2 was isolated and submitted to fragmentation, resulting in an intensive fragment ion with *m/z* 509.304, which was used for quantification (Supplementary Figure S1). Lithium serum concentrations were measured with a commercial polyfluoroporphyrin assay (Funakoshi, Tokyo, Japan) according to manufacturer's instructions.

Behavior analysis. To familiarize animals to the investigator, handling of animals was carried out for five consecutive days prior to start of the experiment. During behavioral testing, cages and animals were randomly selected for testing by a blinded experimenter. All behavior tests were carried out in a dedicated laboratory with soundproof chambers. The Morris water maze task, open field test, elevated plus maze, Porsolt forced-swim test, novelty-induced suppression of feeding and sucrose consumption test were conducted as described previously.[30–32]

Histology. After exsanguination with NaCl animals were transcardially perfused with 4% paraformaldehyde (PFA) solution for 15 min. Subsequent to decapitation, brains were extracted and immediately fixed in 4% PFA at 4 °C. Afterwards brains were washed and kept overnight in 20% sucrose. After dehydration, brains were placed in cryomatrix and frozen in methyl butane at − 50 to − 60 °C.

Immunohistochemistry. Slides were rehydrated through a series of graded ethanol baths and rinsed with phosphate buffered saline (PBS, pH 7.4) prior to 30 min of antigen retrieval at 100 °C in 10 mM sodium citrate buffer pH 6. Unspecific binding sites were blocked with 10% normal goat serum

(NGS) in PBS with 0.1% Triton-X-100 (Sigma-Aldrich) then incubated overnight with rat anti-BrdU antibody (1:500; AbD Serotec, Kidlington, UK) diluted in 10% NGS at 4 °C. In each experiment, a negative control without primary antibody was included. After washing and blocking, secondary biotinylated anti-rat antibody was applied for 2 h (1:250; Life Technologies, Carlsbad, CA, USA) diluted in 10% NGS at room temperature. ABC reagent (Vectastain Elite, Vector Laboratories, Burlingame, CA, USA) was applied for 1 h at a concentration of 9 µl ml^{-1} followed by diaminobenzidine staining (DAB, Sigma-Aldrich) in the presence of 0.01% H_2O_2. One-in-10 series of sections (200 µm apart) from all animals were stained and analyzed.

Immunofluorescence. Slides were treated as mentioned above using the following primary antibodies and dilutions: mouse anti-NeuN biotin conjugated 1:100 (MAB377B, Millipore, Schwalbach, Germany), rabbit anti-Doublecortin 1:250 (ab18723, abcam, Cambridge, UK), rat anti-BrdU 1:500 (OBT0030, AbD Serotec). After washing and blocking, primary antibodies were detected with a fluorophore coupled secondary antibody: Alexa 488-conjugated streptavidin for Biotin-conjugated primaries, goat anti-rabbit IgG Alexa 488, goat anti-mouse IgG Alexa 488, goat anti-rat IgG Alexa 546, goat anti-mouse IgG Alexa 633, goat anti-rabbit IgG Alexa 633 (all 1:250, Life Technologies). Slides were mounted with ProLong Gold antifade reagent with DAPI (Life Technologies).

Cell counts: Cell counts were determined in one-in-10 series of sections covering the entire hippocampus in its rostrocaudal extension. Cell counting was performed by a blinded investigator. Appropriate gain and black level settings were determined on control slices stained with secondary antibodies alone.

Stereology: Postmitotic neurons were NeuN-DAB stained in coronal sections (one-in-10 series, 200 µm apart) of 28 randomly chosen animals ($n = 7$ per group of the PTX/Li$^+$ trial). The absolute cell number was determined by a blinded investigator using a semiautomatic stereology system (Stereo Investigator, MicroBrightField Bioscience, Williston, VT, USA), linked to a Leica DMRE microscope (Leica, Nussloch, Germany).

Data processing, exclusion criteria and statistical analysis. The manuscript was written in accordance with ARRIVE guidelines.[33] Data are presented as mean ± s.e.m. with individual data points or box-whisker-plot (minimum to maximum). All data processing and analysis were completed before unblinding of the analyzer. Data were checked for Gaussian distribution prior to statistical analysis using D'Agostino–Pearson normality test. Statistical analysis was performed using Prism v7.0 (GraphPad Software, La Jolla, CA, USA). Normally distributed data were analyzed using unpaired two-sided *t*-tests (two groups) or ordinary one-way ANOVA with Holm–Sidak *post hoc* analysis for multiple comparisons (⩾3 groups). Analysis of two variables was done by (repeated-measures) two-way ANOVA and *post hoc* analysis of multiple comparisons by controlling the false discovery rate (Benjamini and Hochberg method). Not normally distributed data were analyzed with Mann–Whitney *U* test (two groups). $P < 0.05$ was considered statistically significant and is depicted by an asterisk (NS: not significant). Only statistical outliers that met Peirce's criterion were excluded from the data set.[34,35] Sample size calculation was done prior to execution of *in vivo* experiments based on published effect sizes and expected standard deviations. *In vitro* data including fluorescent-activated cell sorting analysis was obtained from $n = 3$ biological replicates unless stated otherwise.

RESULTS

We used a mouse model of dose-dense PTX therapy where male adult C57Bl/6 mice receive 12 i.p. injections of 20 mg kg^{-1} BW PTX on alternating weekdays over the course of 4 weeks (human equivalent dose of 12×65 mg m^{-2}). The injection protocol (Figure 1a) mimics dose and application frequency of weekly PTX infusions in patients, a paradigm established for instance in breast cancer treatment. We have previously shown that this schedule leads to an axonal-sensory neuropathy but is otherwise well tolerated.[26]

PTX concentrations in different brain regions

PTX is known to reach only low concentrations in the CNS due to active excretion by p-glycoprotein.[36,37] Given that both visuo-spatial and verbal memory abilities largely depend on hippocampal integrity, we were interested if PTX concentrations would differ between various brain regions. We measured PTX concentrations in serum and brain homogenate samples obtained from two animals per time point from 15 min to 12 h after a single i.p. injection of PTX using ultra high-pressure liquid chromatography and tandem mass spectrometry. In line with previous reports,[37] PTX serum concentrations were ~70-fold higher than PTX levels in the brain. Interestingly, PTX concentrations were increased sevenfold in the hippocampus compared with the levels in the neocortex and reached peak concentrations close to 230 nM l^{-1} (Figure 1b).

PTX therapy impairs spatial memory

To test for a possible visuo-spatial impairment, we used the Morris water maze task (MWM), which is based on the paradigm that rodents are able to learn the location of a hidden platform in a swimming pool by memorizing its spatial relation to visual cues.[38] Potentially confounding unspecific toxic effects from PTX treatment were minimized by an 8-days-long recovery period between the last PTX injection and the MWM, which consisted of a 7 days training period (place task) followed by a single probe trial on day 8. PTX-treated animals were slower to learn the location of the hidden platform during training (Supplementary Figure S2A), whereas parameters of motor performance were comparable between PTX and VEH groups. In the concluding spatial probe trial, the platform was removed and the swim patterns of VEH- and PTX-treated mice were recorded (Figure 1c). Animals with previous PTX therapy spent significantly less time and covered less distance in the quadrant that previously contained the platform ($P = 0.039$ (time), respectively, 0.018 (distance); group sizes: $n = 10$ (VEH); $n = 15$ (PTX); unpaired two-sided *t*-test; Figures 1d and e). Importantly, total distance traveled and swim speed were comparable between groups, indicating that PTX-induced neuropathy did not have an impact on water maze performance (Figures 1f and g). As the MWM has a high sensitivity for detecting hippocampus-based spatial cognitive function in rodents,[39] these results suggest that systemic dose-dense PTX therapy might affect hippocampal structures leading to the observed phenotype.

PTX treatment has no effects on affective behavior

Chemotherapy is one potential cofactor for the development of neuropsychiatric sequelae such as anxiety and depression, which is observed in many cancer patients (reviewed by ref. 40). As behavioral changes associated with affective disorders could confound our observations regarding spatial learning, memory and neurogenesis, we conducted a second PTX trial and tested mice for behavioral signs of anxiety, depression or despair. No differences were observed between PTX and VEH-treated mice in monitored movements through a novel open field (Figures 2a and b) or an elevated plus maze (Figure 2c), tests which would indicate increased anxiety. In contrast to typical findings related to anxiety in a conflicting forced-choice situation, we recorded a small but significant decrease in the feeding latency of the PTX group in the novelty-induced suppression of feeding test ($P = 0.048$; group sizes: $n = 15$ (VEH) and $n = 13$ (PTX); unpaired two-sided *t*-tests; Figure 2d). Furthermore, PTX-treated mice neither showed signs of despair in their response to a desperate situation (Porsolt forced-swimming test; Figure 2e) nor anhedonic behavior (sucrose consumption test; Figure 2f). In summary, we did not detect any relevant alterations of affective behavior in mice after PTX treatment.

PTX induces cytotoxicity in NSC through a calpain- and caspase-mediated mechanism

It was previously shown that a reduction of hippocampal adult neurogenesis leads to impaired spatial learning and memory.[41,42] Considering our behavioral observations and that PTX levels were

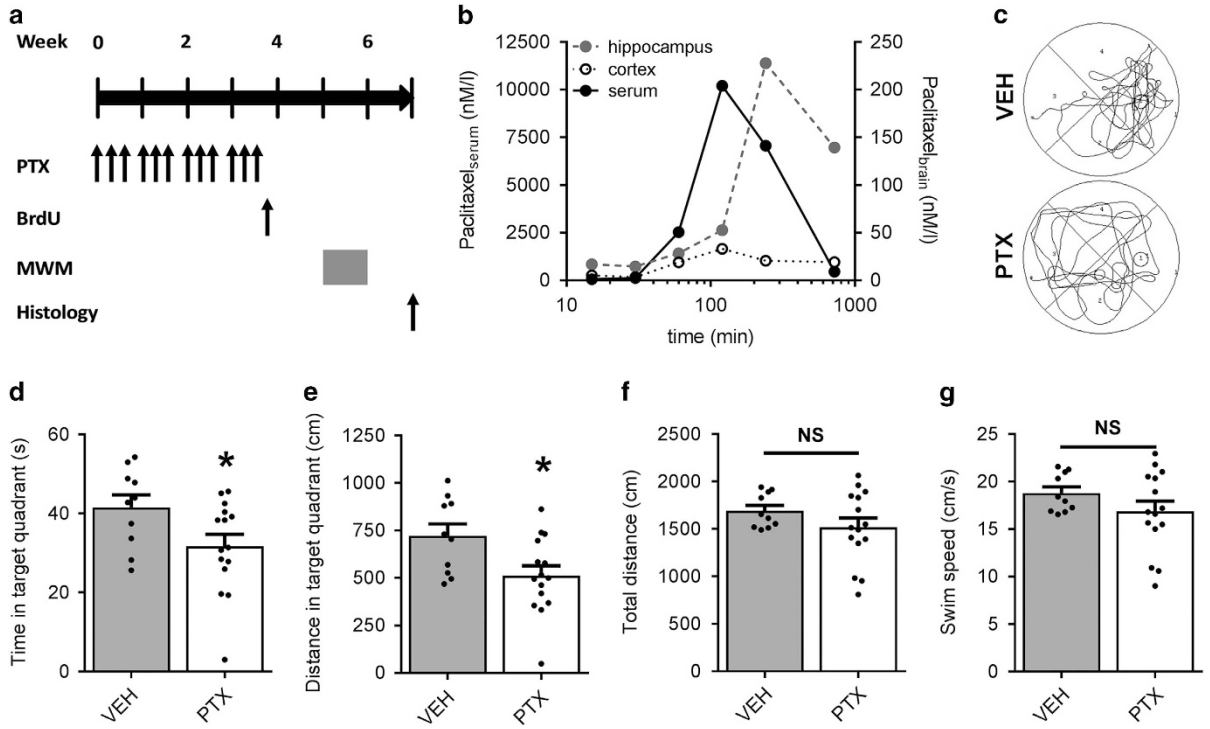

Figure 1. Effects of dose-dense paclitaxel (PTX) treatment on spatial memory. (**a**) Schedule of dose-dense PTX treatment and the Morris water maze (MWM) experiment. Animals received a total of 12 intraperitoneal (i.p.) PTX injections with 20 mg kg^{-1} BW each (three times per week over the course of 4 weeks). Animals were allowed to rest for 8 days prior to training in the MWM. (**b**) PTX serum and tissue concentrations at 15, 30, 60, 120, 240 and 720 min after single i.p. PTX injection with 20 mg kg^{-1} body weight (BW): serum levels (left *y* axis) were almost two orders of magnitude higher compared with the brain concentrations (right *y* axis). In the brain, PTX levels measured in the hippocampus were approximately sevenfold higher than those measured in the neocortex. (**c**) In the MWM, PTX-treated mice performed worse in the probe trial: representative images of swim patterns from a VEH- and PTX-treated mouse. (**d**) Compared to controls, PTX-treated mice spent significantly less time and (**e**) swam significantly shorter distances in the target quadrant, whereas (**f**) the overall distances covered and (**g**) swim speed were comparable. Statistical analysis: (**b**) No statistical analysis was performed ($n=2$ per time point). (**d**–**g**) Data were checked for normal distribution using D'Agostino–Pearson normality test and thereafter analyzed using unpaired two-sided *t*-tests (group sizes: $n=10$ (VEH); $n=15$ (PTX)). *$P<0.05$; NS, not significant.

higher in the hippocampus than in the neocortex, we hypothesized that cognitive deficits after PTX therapy could be attributed to an impaired hippocampal neurogenesis. We therefore examined effects of PTX on cultured mouse NSC *in vitro*. In our pharmacokinetics profile, PTX concentrations peaked at 2 h (serum) and 4 h (brain) post injection, respectively. We therefore chose a more conservative timeframe of 2 h PTX exposure for our experiments. When we exposed NSC with various PTX concentrations ranging from 3 pM to 3 μM for 2 h, we observed severe cytotoxicity even in the low nanomolar concentration range, despite the short exposure time (Supplementary Figure S3a). The calculated EC_{50} for NSC in the dose–response curve was 27 nM (non-linear regression fit; Figure 3a). Human neuronal progenitor cells (hNPC) derived from induced pluripotent stem cells (iPSC) were equally sensitive with a calculated EC_{50} of 4 nM (non-linear regression fit; Figure 3a). In contrast to NSC and hNPC, mouse mature HCN were less susceptible to the same treatment with a calculated EC_{50} of 4700 nM (non-linear regression fit; Figure 3a). As the division rate of adult NSC is low compared to malignant cells, we considered it unlikely that the observed severe cytotoxicity in NSC could solely be attributed to PTX' cytostatic properties, which are only exerted during the M-phase of the cell cycle. In our NSC cultures, we observed an average cycle time of 2.3 days, which is in line with previously published data.[43] In a next step, we measured the percentage of NSC in the G2/M-phase. After 2 h exposure to VEH or PTX, only 6.1% of VEH- and 7.6% of PTX-treated cells were in the G2/M-phase (not significant; Figure 3b), whereas the largest portion of cells were in the G1-phase. On the basis of the previously established dose–response curve, we chose a 30 nM PTX dose for subsequent experiments, which reduced cell viability to 48 ± 5% compared with VEH-treated controls. The ratiometric calcium (Ca^{2+}) indicator Fura-2 was used to assess cytoplasmic baseline Ca^{2+} levels after PTX treatment. In PTX-treated cells compared with VEH exposed controls, we observed a significantly higher λ340/380 nm excitation ratio ($P<0.0001$; $n=53$ (PTX), $n=68$ (VEH) cells, five replicates; two-sided *t*-test; Figure 3c). We next investigated apoptotic cell death as a possible mechanism. When we measured activity of the executioner caspases 3/7 at different time points, we observed a marked increase of activity 12 h post PTX treatment ($P\leqslant0.0001$; $F(3, 24)=14.32$; ordinary one-way ANOVA; Figure 3d). Notably, the calculated EC50 for caspase 3/7 activation was 16 nm (non-linear regression fit, Figure 3e). We next tested caspases upstream of caspase 3/7 and also observed an increase of caspase 9 activity (Figure 3e).

In regards to the observed increase of baseline Ca^{2+} levels after PTX treatment, we have previously demonstrated, that PTX can bind to the protein neuronal calcium sensor-1 (NCS-1), increasing positive modulation of the inositol 1,4,5-trisphosphate receptor ($InsP_3R1$) and causing elevated levels of intracellular Ca^{2+} .[44] In dorsal root ganglia sensory neurons (DRGN), this increase of Ca^{2+} is sufficient to activate the Ca^{2+}-dependent protease calpain[25] and thereby contributes to the development of a PTX-induced peripheral neuropathy. We hypothesized, that the same

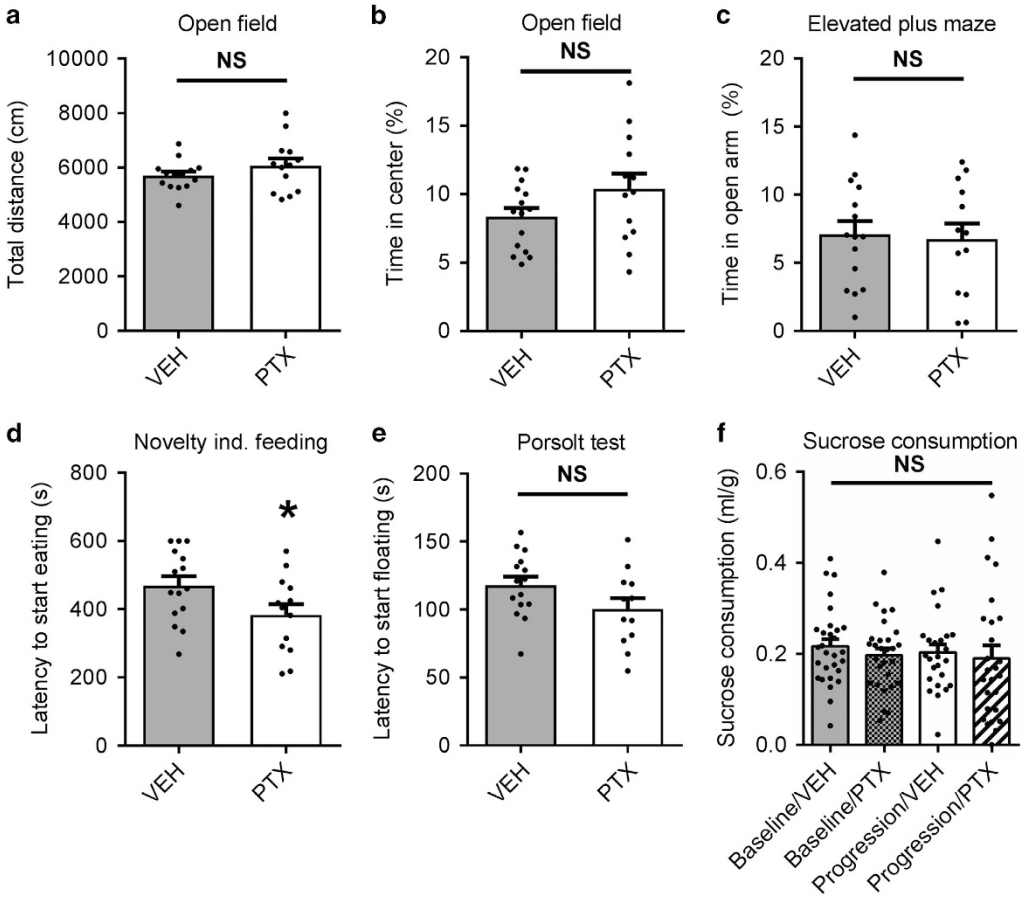

Figure 2. Paclitaxel (PTX) has no effect on anxiety and depression related behavior. (**a**) Dose-dense PTX treatment affected neither the total distance traveled nor (**b**) the time spent in the center of a novel open field. (**c**) PTX and vehicle (VEH)-treated animals spent a comparable amount of time in the open arms of an elevated plus maze. (**d**) Animals treated with PTX showed a small but significant decrease in the latency to start eating in a novel environment, whereas (**e**) latency to start floating in the Porsolt forced-swim test and (**f**) sucrose consumption per body weight was comparable between groups. Statistical analysis: data were checked for normal distribution using D'Agostino–Pearson normality test and thereafter analyzed using (**a**–**e**) unpaired two-sided *t*-tests (group sizes: $n = 15$ (VEH) and $n = 13$ (PTX)) and (**f**) repeated-measures two-way ANOVA and Benjamini and Hochberg *post hoc* test (group sizes each: $n = 27$). *$P < 0.05$; NS not significant.

mechanism might initiate caspase activation and cell death in NSC and that cell-specific expression of NCS-1, respectively, $InsP_3R1$ may lead to differential effects on various cell types. When we tested protein expression levels of NCS-1, we observed a strong expression in cultured NSC but not HCN or in a human breast cancer cell line (MCF-7). NSC additionally showed stronger protein expression levels of the $InsP_3R1$ compared with HCN (Figure 3f). Measurements of calpain activity in NSC revealed a significant increase as early as 1 h after PTX exposure, which could be inhibited with the calpain inhibitor MDL28170 ($P < 0.0001$; $F_{(3, 26)} = 29.68$; ordinary one-way ANOVA; Figure 3g and Supplementary Figure S3F). We previously established that the interaction of NCS-1 with the $InsP_3R1$ can be specifically inhibited with lithium ions (Li^+).[45] Further assessment of caspase 3/7 activity showed that the PTX-induced increase of caspase 3/7 activity was inhibited by co-treatment with a caspase 3/7 inhibitor (AC-DEVD-CHO), with the calpain inhibitor MDL28170 and Li^+ ($P < 0.0001$; $F_{(5, 48)} = 52.02$; ordinary one-way ANOVA; Figure 3d and Supplementary Figure S3G). However, A1070722, a selective inhibitor of glycogen synthase kinase 3 beta (GSK3β), which is a known molecular target of Li^+, had no effect (Figure 3d). We next tested whether interference with intracellular Ca^{2+} signaling would affect cell viability after PTX exposure. Inhibition of calpain, but more effectively co-treatment with Li^+, restored decreased cell viability of PTX exposed NSC to almost control levels ($P < 0.0001$; $F_{(5, 30)} = 112.7$; ordinary one-way ANOVA; Figure 3h and Supplementary Figures S3B, S3D and S3E), whereas inhibition of GSK3 had no influence. Albeit not significant, cell viability of PTX/Li^+-treated NSC was still slightly reduced by 16% compared with VEH treatment, which might be explained by PTX' cytostatic mechanism of action towards NSC. In comparison to the observations in NSC, malignant cells from the human breast cancer cell line MCF-7 and cervical cancer cell line HeLa, were less sensitive to PTX and were not protected by lithium co-medication (Figure 3i). Taken together, our results suggest that observed PTX concentrations in the hippocampus after systemic application are sufficient to induce cell death in NSC independent of cell cycle status. Owing to the short exposure time and the vulnerability of NSC, cytotoxicity in this condition appears to be mediated mainly by Ca^{2+} and caspase-dependent mechanisms and only to a much lesser extent by PTX' effects on the microtubule cytoskeleton.

Lithium co-treatment prevents PTX-induced cognitive changes

To test the hypothesis that co-treatment with Li^+ prevents PTX-mediated toxicity towards NSC and progenitor cells, and that NSC toxicity could be relevant for the development of visual-spatial deficits, we studied the efficacy of preventive Li^+ application in PTX therapy. Animals were randomly assigned to four groups and injected either with 12.8 mg kg^{-1} BW Li^+ or sodium chloride (VEH)

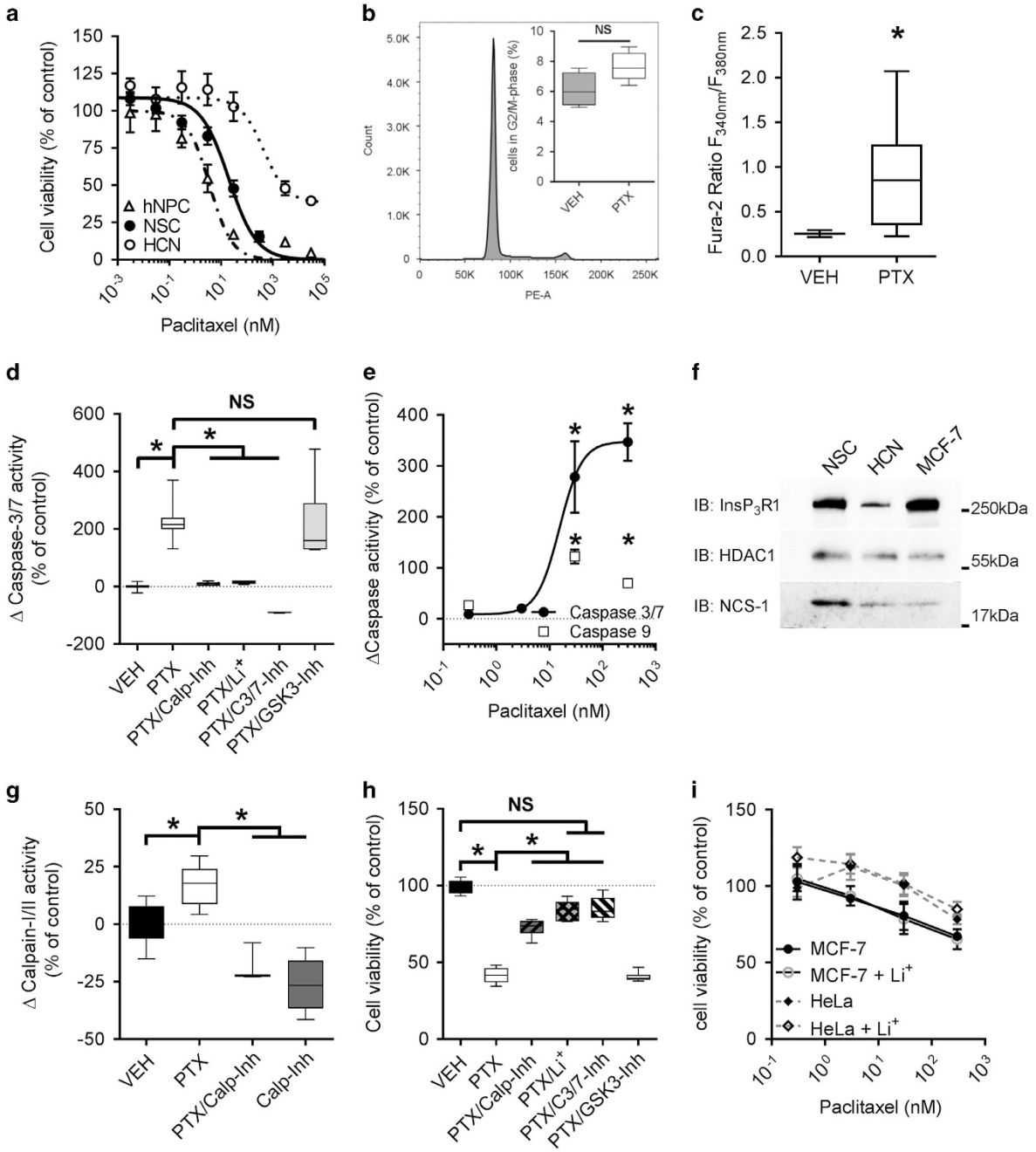

Figure 3. Paclitaxel (PTX)-induced cytotoxicity in neural stem cells (NSC). (**a**) Dose–response curve of cytotoxicity in mouse NSC (black dots), induced pluripotent stem cells (iPSC)-derived human neuronal progenitor cells (hNPC, open triangle) and post-mitotic mouse hippocampus neurons (HCN; clear dots) after 2 h exposure time with PTX. Data were fitted with a three-parameter logistic curve. (**b**) Representative histogram of cell cycle analysis in NSC. After both vehicle (VEH), respectively, PTX treatment, only small percentages of NSC were in G2/M-phase (insert). (**c**) Treatment of NSC with 30 nM PTX led to a significant increase in resting Ca^{2+} levels, evidenced by a higher Fura-2 excitation ratio. (**d**) Caspase-3/7 activity was significantly increased after PTX treatment (30 nM) and was inhibited by co-incubation with the calpain inhibitor MDL28170 (Calp-Inh; 10 μM), lithium chloride (Li^+; 1 mM), and the caspase inhibitor AC-DEVD-CHO (C3/7-Inh; 1 μM). Caspase-3/7 activity remained high after co-treatment with the GSK3β inhibitor A1070722 (GSK3-Inh; 100 nM). (**e**) Dose–response curve of caspase 3/7 (closed circles) and caspase 9 (open squares) activity in NSC 12 h after 2 h exposure with different PTX concentrations. (**f**) Protein expression of NCS-1 is higher in NSC compared with HCN and MCF-7 breast cancer cells. (Loading control of whole cell lysates: HDAC-1). (**g**) PTX induces an increase in calpain activity which could be prevented with the calpain inhibitor MDL28170 (Calp-Inh; 10 μM). (**h**) Impaired cell viability of NSC after exposure to 30 nM PTX was significantly improved by co-incubation with MDL28170 (Calp-Inh; 10 μM), Li^+ (1 mM) or AC-DEVD-CHO (C3/7-Inh; 1 μM), respectively, but not with the GSK3β inhibitor A1070722. (**i**) Exposure of MCF-7 and HeLa cells to different PTX concentrations for 2 h with and without 1 mM Li^+ did not show a protective effect for the lithium co-medication in these cancer cell lines. Statistical analysis: data were checked for normal distribution using D'Agostino–Pearson normality test and then analyzed using (**b**) Mann–Whitney *U* test, (**c**) unpaired two-sided *t*-test and (**d-e** and **g–i**) ordinary one-way ANOVA and Holm–Sidak *post hoc* test (data are obtained from $n = 3$ individual experiments with 4–6 technical replicates for each condition). *$P < 0.05$; NS, not significant.

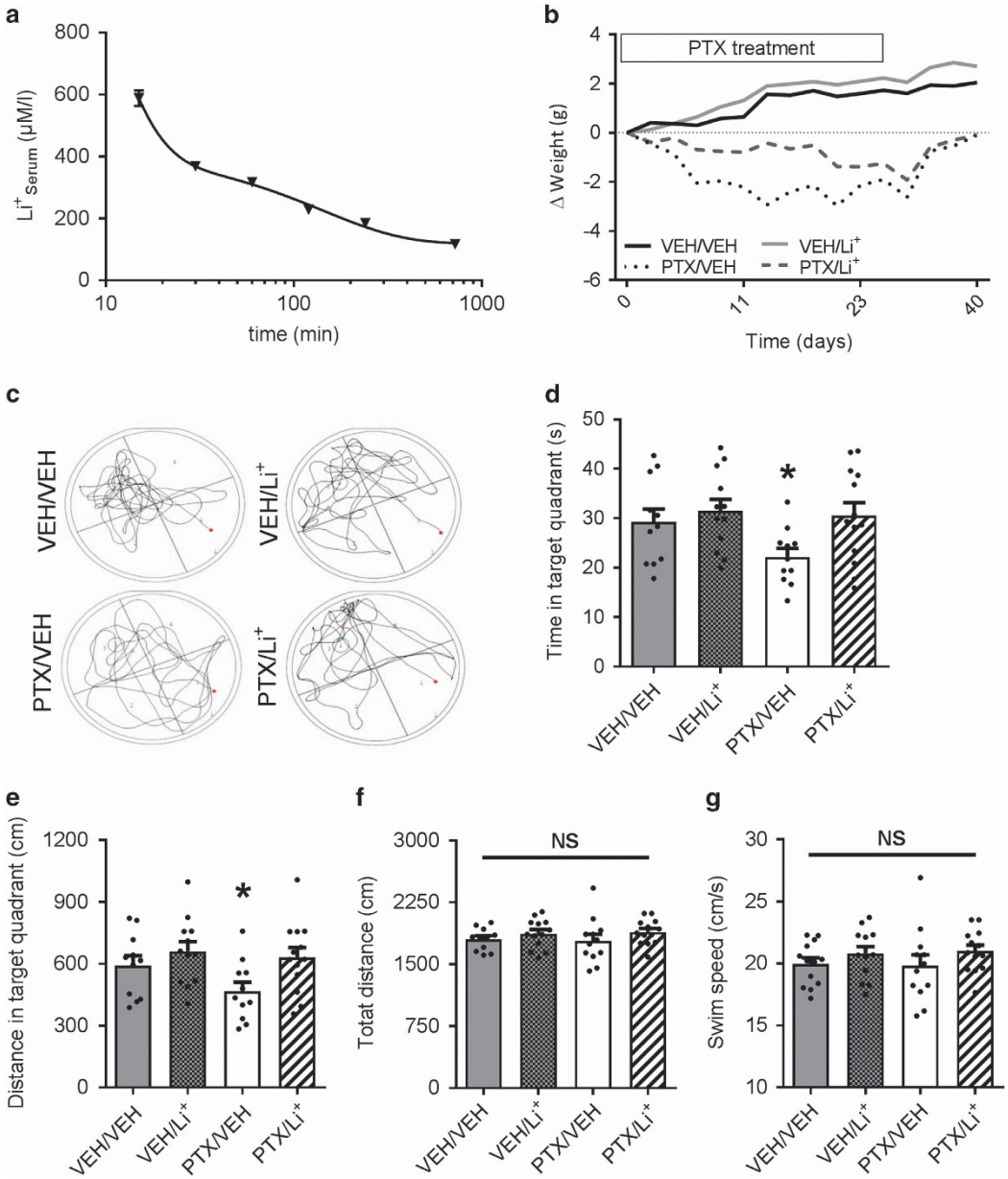

Figure 4. Effects of Li^+ on paclitaxel (PTX)-induced cognitive deficits. In a first step, the pharmacokinetics of Li^+ was assessed: (**a**) Li^+ serum concentrations were measured after a single intraperitoneal (i.p.) injection with 12.8 mg kg^{-1} BW lithium carbonate. The observed decay is consistent with a two-compartment model. Next, four groups of animals were treated with PTX or vehicle (VEH) and Li^+ or the respective VEH. (**b**) PTX/VEH-treated animals (gray dotted line) had a moderate but significant weight loss compared with VEH/VEH-treated animals (black solid line), which was less pronounced in the PTX/Li^+ group (gray dashed line). Duration of PTX treatment is marked by bar above the graph. (**c**) Representative swim patterns of VEH/VEH, VEH/Li^+, PTX/VEH and PTX/Li^+-treated mice recorded in the probe trial of the MWM task, in which (**d**) PTX/VEH-treated animals spent significantly less time and covered (**e**) less distance in the target quadrant compared with the PTX/Li^+ and VEH groups whereas (**f**) overall distance covered and (**g**) swim speed was similar between the groups. Statistical analysis: data were checked for normal distribution using the D'Agostino–Pearson normality test and then analyzed using (**d**–**g**) ordinary two-way ANOVA and Benjamini and Hochberg *post hoc* test (group sizes: $n = 11$ (VEH/VEH): $n = 13$ (PTX/Li^+); $n = 11$ (PTX/VEH); $n = 12$ (VEH/Li^+)). *$P < 0.05$; NS, not significant.

15 min prior to every application of PTX or VEH. This previously established dose[46] yielded non-toxic serum levels in the high micromolar dose range (Figure 4a). The treatment was generally well tolerated with normal spontaneous behavior observed in all treatment groups, however 4 out of 60 animals died due to injection related complications (2 VEH/Li^+; 1 PTX/VEH; 1 PTX/Li^+). Mice in the PTX/VEH, and to a lesser extent in the PTX/Li^+ group, showed a moderate weight loss during therapy, which rapidly recovered after the last injection (Figure 4b). Similar to our pilot trial, we observed longer latencies for mice of the PTX/VEH group to locate the hidden platform during MWM training (Supplementary Figure S2B). The same pattern was maintained in the probe trial: PTX/VEH injected mice took longer to locate the former position of the platform (data not shown), spent significantly less time in the target quadrant ($P = 0.03$; $F_{(1, 43)} = 4956$; ordinary two-way ANOVA and Benjamini and Hochberg

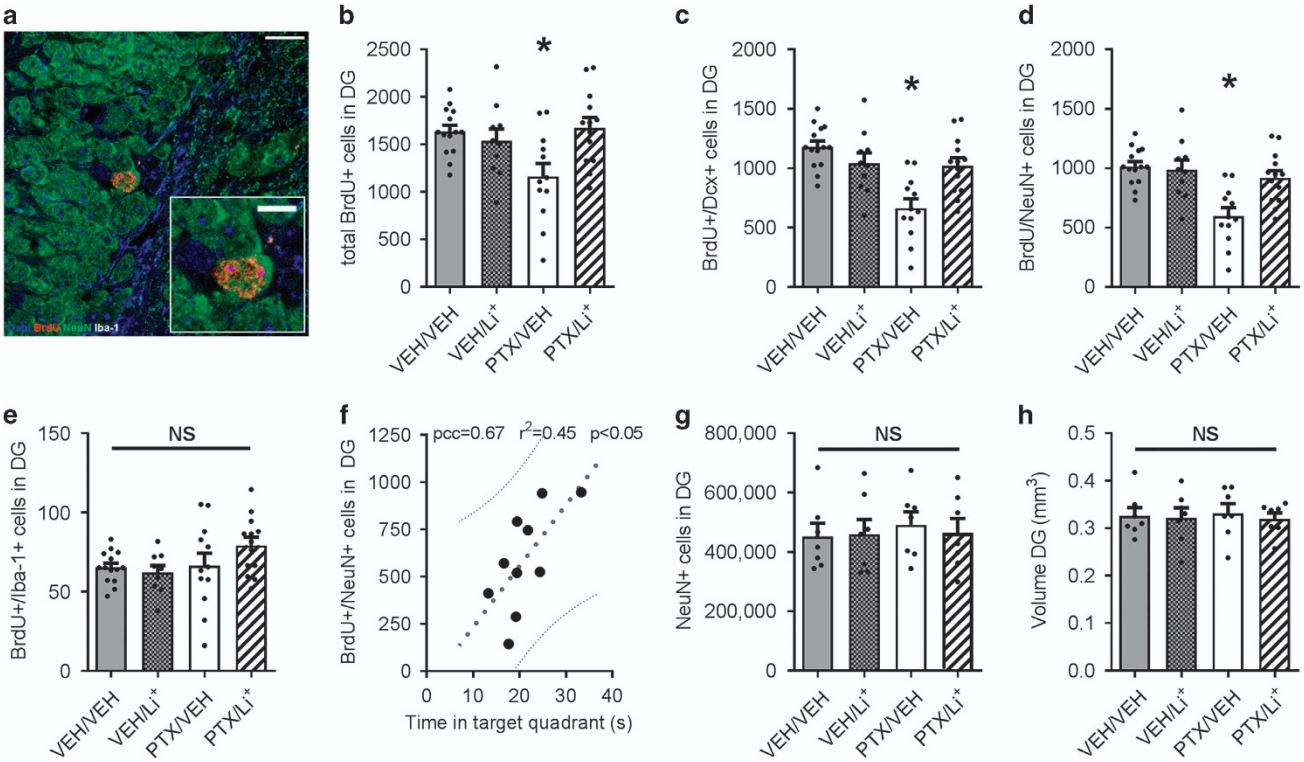

Figure 5. Neurogenesis in the dentate gyrus of the hippocampus is affected by paclitaxel (PTX) therapy. (**a**) Representative image of 5-Bromo-2′-deoxyuridine (BrdU)-positive cells in the dentate gyrus (DG) co-expressing the mature neuronal marker NeuN; scale bar is 10 μm. Insert shows enlarged image of BrdU/NeuN-positive cell (scale bar is 5 μm). (**b**) PTX/VEH-treated animals had significantly fewer BrdU-positive cells compared with VEH/VEH and PTX/Li^+ treatment groups and (**c**) the number of newly generated immature neurons (BrdU+/Dcx+) was significantly reduced in the PTX/VEH group only, whereas Li^+ application prevented these changes. (**d**) Further phenotyping of BrdU-positive cells revealed that in the PTX/VEH group significantly fewer cells were positive for NeuN. (**e**) Cell counts for BrdU-positive microglia cells (BrdU +/Iba-1+) were comparable across all groups. (**f**) The number of BrdU/NeuN-positive cells in the PTX/VEH group correlated positively with water maze performance during the probe trial. (**g**) Stereological counting showed similar total numbers of NeuN+ cells in the DG region. (**h**) Analysis of the dentate gyrus volume showed no evidence of hippocampal shrinkage in PTX-treated groups. Statistical analysis: data were checked for normal distribution using D'Agostino–Pearson normality test and then analyzed using ordinary two-way ANOVA and Benjamini and Hochberg *post hoc* test (group sizes: (**b**–**e**): $n = 14$ (VEH/VEH); $n = 13$ (PTX/Li^+); $n = 12$ (PTX/VEH); $n = 10$ (VEH/Li^+); (**g**, **h**) group sizes $n = 7$ (all groups)). (**f**) Pearson correlation coefficient and 95% confidence band was calculated between BrdU/NeuN-positive cells and Morris water maze performance for $n = 10$ animals of the PTX/VEH group. *$P < 0.05$; NS, not significant.

post hoc test; group sizes: $n = 11$ (VEH/VEH), $n = 13$ (PTX/Li^+); $n = 11$ (PTX/VEH); $n = 12$ (VEH/Li^+); Figures 4c and d) and covered a shorter distance in the target quadrant ($P = 0.02$; $F_{(1,\ 43)} = 6072$; ordinary two-way ANOVA and Benjamini and Hochberg *post hoc* test; group sizes: $n = 11$ (VEH/VEH), $n = 13$ (PTX/Li^+); $n = 11$ (PTX/VEH); $n = 12$ (VEH/Li^+); Figure 4e). Animals which received PTX and the preventive intervention with Li^+ performed equally well compared with the control groups (Figures 4c–e), and all animals covered comparable total distances and showed similar swim speeds (Figures 4f and g). Taken together, our results suggest that preemptive co-treatment with Li^+ prevents PTX-induced changes of visual-spatial function in rodents.

PTX treatment alters adult neurogenesis of the dentate gyrus

In a next step we were interested, if increased cell death of resident NSC affects hippocampal cell proliferation and neuronal differentiation *in vivo*. Therefore, we injected a pulse of BrdU, a nucleoside analog that is taken up into the DNA of replicating cells during S-phase,[47] 24 h after the last PTX treatment in the Li^+ intervention trial. Analysis revealed fewer BrdU-positive cells in the dentate gyrus (DG) of the PTX/VEH group ($P = 0.0083$; $F_{(1,\ 45)} = 7616$; ordinary two-way ANOVA and Benjamini and Hochberg *post hoc* test; group sizes: $n = 14$ (VEH/VEH); $n = 10$ (VEH/Li^+), $n = 13$ (PTX/Li^+); $n = 12$ (PTX/VEH); Figures 5a and b), whereas PTX/Li^+ and VEH/VEH-treated mice showed comparable numbers. When we tracked these stem and progenitor cells by colocalization with other markers, we observed a decrease of immature neuronal cells (BrdU/doublecortin positive cells (BrdU+/Dcx+); $P = 0.0001$; $F_{(1,\ 45)} = 128$; ordinary two-way ANOVA and Benjamini and Hochberg *post hoc* test; group sizes: $n = 14$ (VEH/VEH); $n = 10$ (VEH/Li^+), $n = 13$ (PTX/Li^+); $n = 12$ (PTX/VEH); Figure 5c) in the PTX/VEH group only. We also detected fewer newly generated mature neurons (BrdU/NeuN-positive cells; $P = 0.0076$; $F_{(1,\ 45)} = 7818$; ordinary two-way ANOVA and Benjamini and Hochberg *post hoc* test; group sizes: $n = 14$ (VEH/VEH); $n = 10$ (VEH/Li^+), $n = 13$ (PTX/Li^+); $n = 12$ (PTX/VEH); Figure 5d) after PTX but not Li^+ treatment, whereas the number of BrdU/Iba-1 double positive microglia was comparable between the four groups (Figure 5e). Interestingly, we observed a positive statistical correlation between the number of BrdU-positive neurons and water maze performance in the probe trial after PTX/VEH treatment (Pearson correlation coefficient (pcc) = 0.67; $n = 10$ animals; Figure 5f). In the other treatment groups, this kind of correlation did not reach statistical significance. As PTX-induced cell death of pre-existing post-mitotic neurons in the hippocampal formation could also account for our behavioral phenotype, we performed stereological cell counting of post-mitotic mature neurons (NeuN) in the DG and Cornu ammonis 3 (CA3) region. Our obtained calculations for total cell count and

volume were comparable with previous literature.[48] In this analysis, we did not detect any differences in the total number of neurons in the DG (Figure 5g) and CA3 region (data not shown) between the four groups, nor a difference in DG volume (Figure 5h). The lack of difference in absolute NeuN-positive cells, despite of a reduced neurogenesis after PTX therapy, is most likely due to a lack of sensitivity of this method with a comparatively high inherent variance. Nonetheless, this finding underlines our observations in cultured cells, which suggest that HCN are much less sensitive to PTX than NSC.

In summary, these findings agree with our *in vitro* data, which point to an increased vulnerability of neural stem and progenitor cells to PTX. Moreover, we were able to show that preemptive Li^+ treatment prevents PTX-induced behavioral and histological changes.

DISCUSSION

Up to 50% of patients undergoing systemic chemotherapy report cognitive impairment in temporal correlation to therapy.[49] In spite of the high incidence of cognitive dysfunction reported after chemotherapy, the performance in neuropsychological tests frequently correlates poorly with patients' subjective perception resulting in a great heterogeneity of the clinical data (reviewed by refs 50–53). However, preclinical findings (reviewed by ref. 54) and the structural changes observed in imaging studies[55] suggest a neurobiological basis for PCCI. This interpretation is supported by a growing number of preclinical studies, which report cognitive changes for instance in mice treated with 5-fluoruracil and oxaliplatin[56] and rats following treatment with a taxane (for example, refs 15–17). The impaired spatial memory in the MWM task detected in our mouse model of dose-dense paclitaxel-therapy differs from the reported normal water maze performance in rats treated with 4×2 mg kg^{-1} BW PTX,[15] suggesting a dose-dependent effect. In a clinical meta-analysis of PCCI in patients suffering from breast cancer, small to moderate changes in visuo-spatial memory were observed,[3] similar to the effect size we report in our experiments. PTX therapy was not a criterion of this meta-analysis although breast cancer patients are frequently treated with PTX. Further clinical studies with cohorts receiving defined cytostatic drugs such as PTX are thus needed and are presently under way (for example, CICARO study, NCT02753036).

Our results of PTX serum and brain concentrations are comparable to a previous study in CD2F1 mice.[37] However, this study did not distinguish between concentrations in various brain regions. We believe we demonstrate for the first time, that PTX levels in the hippocampus are higher compared with the neocortex, making the hippocampus particularly prone to PTX-induced neurotoxicity. The molecular mechanism underlying regional differences in PTX concentrations remains unclear: as paclitaxel is a highly lipophilic drug, which can cross biological membranes by passive diffusion processes, one speculative hypothesis could be differences in efflux mechanisms such as p-glycoprotein. Further studies are needed to establish whether this observation is specific for paclitaxel, elucidate underlying mechanism and to assess pharmacokinetic properties of repeated dosing experiments. The finding of uneven brain distribution of PTX correlates well with our observations *in vivo,* were reduced numbers of stem and progenitor cells in the DG of the hippocampus were counted. Furthermore, PTX concentrations in the hippocampus were more than sufficient to induce marked cytotoxicity in cultured adult NSC *in vitro*. In fact, the observed toxicity of PTX against NSC in our paradigm is quite severe compared with the published results obtained in malignant cells, where only a small fraction of cells died when exposed to nanomolar PTX concentrations for 2 h.[57,58] IPSC-derived hNPC were equally sensitive to PTX, supporting a potential clinical relevance in patients. This observation is intriguing, as PTX' main cytostatic mode of action is by stabilization of the microtubule cytoskeleton,[59] whereas the observed pathomechanism in NSC involving Ca^{2+} signaling is independent of the cell cycle state and appears similar to mechanisms of damage in DRGN.[25] In this scenario, PTX stabilizes the Ca^{2+} bound conformation of NCS-1,[44] which is known to positively modulate the $InsP_3R1$ located in the endoplasmic reticulum.[45] The resulting increase in intracellular Ca^{2+} is sufficient to activate the Ca^{2+}-dependent protease calpain[25] and trigger 'direct' cell death by activation of caspases downstream of calpain (simplified model summarized in Supplementary Figure S4). One aspect of this model is, that the observed differences in susceptibility to PTX between cell types can, at least in part, be explained by variations of protein expression levels. In the present study for instance NSC showed much higher levels of both $InsP_3R1$ and NCS-1 compared with HCN and in previous studies differential effects in cardiomyocytes compared with the observations made in DRGN, could be attributed to differences in calpain expression.[60] Although this mechanism appears intriguing, it has to be considered that calpains have very diverse cellular substrates and can mediate other cell death mechanisms including necrosis (reviewed by ref. 61). Apart from cytotoxicity calpains were also shown to have an important role in synaptic plasticity by mediating both post-translational modifications as well as changes in gene expression (reviewed by ref. 62), with important implications for different pathologies including Alzheimer disease.[63] Another possibility is that the targets of calpains actually depend on the amplitude of the stress, for example, a higher dose of PTX leads to activation of caspases when the cell is unable to cope with the stress, whereas lower doses activate other targets. Indeed it was previously shown, that very high (10 μM) doses of paclitaxel induce an opening of the mitochondrial permeability transition pore,[64] whereas doses in the nanomolar dose range induce NCS-1 and InsP3R1-mediated effects.[44] The present study uses low paclitaxel concentrations close to the EC_{50} of NSC, which are sufficient to activate caspases. Although it is possible that even lower concentrations would induce differential effects, they do not appear to alter cell viability in our model. To further strengthen the proposed molecular sequence, it would be useful to target the proposed molecular mechanism at several stages simultaneously and check for additive, respectively, synergistic effects. However, treating cell models with a combination of pharmacological inhibitors is challenging, as specificity and potential interactions are a great concern when using multiple pharmacological interventions. As a result, combining different substances often yields unpredictable results. Ideally, inducible genetic approaches were to be combined with pharmacological interventions in future experiments.

Previously published observations suggest that Li^+ binds NCS-1, thus blocking the positive modulation of the $InsP_3R1$ and preventing apoptosis in DRGN.[65] We used Li^+ application to prevent PTX-induced cell death of NSC *in vitro*, and furthermore, to restore spatial memory performance and normalize adult hippocampal neurogenesis *in vivo*. However, given the vast literature on biological effects of Li^+ (a 2016 Medline query for 'lithium' lists more than 45 000 publications), alternative mechanisms underlying paclitaxel-induced neurotoxicity cannot be entirely precluded. One possibility is inhibition of glycogen synthase kinase 3 (GSK3) by Li^+, which was shown to have an important role in PTX-induced neuropathic pain,[66] as well as inhibition of microglia activation, and reduction of pro-inflammatory cytokines such as interleukin-6, which have been linked to PCCI.[67] In our cell culture model of NSC however, inhibition of calpain but not GSK3 prevented PTX-induced toxicity, supporting the hypothesis of a Ca^{2+}-dependent mechanism. Interestingly, a similar observation was made previously, when Li^+ was tested as a preventive medication in dorsal root ganglion neurons.[46] Another possibility in regards to PTX-mediated neurotoxic effects could be neurophysiological changes exerted

for instance on hippocampal synaptic function. This possibility appears however unlikely, as cerebrospinal fluid concentrations of 10 μM PTX (50 times the concentrations observed in our study in hippocampal tissue) did not elicit clear alterations of hippocampal synaptic function in an *in vivo* rat model.[68] Yet another possibility is that PTX-induced cell death is ameliorated by an enhanced Li^+-mediated neurogenesis[69] with increased neuronal differentiation of progenitor cells.[70] These effects were shown to be neuroprotective in other conditions such as Huntington's disease[71] and hypoxia–ischemia.[72] In contrast to the aforementioned study that used continuous Li^+ treatment over 4 weeks, mice were injected only 12 times in our paradigm. Given the relatively short half-life of Li^+ in rodents,[73] the absence of a measurable increase of BrdU-positive neuronal cells in Li^+-treated control animals and the fact that Li^+ dosages in our study were almost an order of magnitude lower, an effect based solely on proliferation/differentiation induced by Li^+ seems very unlikely. Presently, Li^+ is used for different psychiatric conditions with desired serum concentrations of 0.6–1.2 mM l^{-1}. Although its pharmacology is challenging, it has been thoroughly characterized and therefore would not present an obstacle for clinical translation (reviewed by ref. 74). Importantly, in our animal model lithium serum levels of up to 0.6 mM l^{-1} proved to be effective in the prevention of paclitaxel-induced neurotoxicity and were well below toxic concentrations which start above 1.5 mM l^{-1}. In the context of a potential use in cancer patients, the question of whether Li^+ reduces PTX' cytostatic efficacy is a key issue. To this point, no detrimental effect of Li^+ on the antineoplastic effects of PTX has been observed *in vitro* or in a tumor transplant model,[46] but additional preclinical and clinical studies are needed to address this question.

In conclusion, we report that dose-dense PTX therapy in mice leads to death of neuronal stem and progenitor cells in the hippocampus and impaired spatial memory. As the measured PTX concentrations in the CNS were low and only a small percentage of NSC were in the G2/M-phase of the cell cycle, only a small fraction of the observed cell death can be attributed to the tubulin-dependent cytostatic properties of PTX. PTX-induced toxicity against NSC appears to be mainly caused by a Ca^{2+}-dependent molecular mechanism involving the proteins NCS-1 as well as $InsP_3R1$. Targeting this mechanism with Li^+ co-treatment reduced toxicity *in vitro*, and prevented behavioral and histological alterations *in vivo*. As a result, a new strategy for the clinical prevention of PTX-induced neurotoxicity in the central and peripheral nervous emerges, which has the potential to change clinical practice.

CONFLICT OF INTEREST

The authors declare no conflict of interest.

ACKNOWLEDGMENTS

We thank Petra Loge for excellent technical assistance and Catherine Aubel for help in text editing. We thank Dr Harald Stachelscheid (BIH Stem Cell Core Facility) for neuronal progenitor cells derived from iPSC. The research leading to these results has received funding from the Federal Ministry of Education and Research via the grant Center for Stroke Research Berlin (01 EO 0801) and from the Deutsche Forschungsgemeinschaft (EXC 257 NeuroCure). PH and WB receive stipends from the Charité Clinician Scientist Program funded by the Charité Universitätsmedizin Berlin and the BIH.

REFERENCES

1 Kerckhove N, Collin A, Conde S, Chaleteix C, Pezet D, Balayssac D. Long-term effects, pathophysiological mechanisms, and risk factors of chemotherapy-induced peripheral neuropathies: a comprehensive literature review. *Front Pharmacol* 2017; **8**: 86.
2 Joly F, Giffard B, Rigal O, De Ruiter MB, Small BJ, Dubois M *et al.* Impact of cancer and its treatments on cognitive function: advances in research from the paris international cognition and cancer task force symposium and update since 2012. *J Pain Symptom Manage* 2015; **50**: 830–841.
3 Jim HS, Phillips KM, Chait S, Faul LA, Popa MA, Lee YH *et al.* Meta-analysis of cognitive functioning in breast cancer survivors previously treated with standard-dose chemotherapy. *J Clin Oncol* 2012; **30**: 3578–3587.
4 Stewart A, Bielajew C, Collins B, Parkinson M, Tomiak E. A meta-analysis of the neuropsychological effects of adjuvant chemotherapy treatment in women treated for breast cancer. *Clin Neuropsychol* 2006; **20**: 76–89.
5 Ahles TA, Saykin AJ. Candidate mechanisms for chemotherapy-induced cognitive changes. *Nat Rev Cancer* 2007; **7**: 192–201.
6 Zeller B, Tamnes CK, Kanellopoulos A, Amlien IK, Andersson S, Due-Tonnessen P *et al.* Reduced neuroanatomic volumes in long-term survivors of childhood acute lymphoblastic leukemia. *J Clin Oncol* 2013; **31**: 2078–2085.
7 Deeken JF, Loscher W. The blood-brain barrier and cancer: transporters, treatment, and Trojan horses. *Clin Cancer Res* 2007; **13**: 1663–1674.
8 Myers JS, Pierce J, Pazdernik T. Neurotoxicology of chemotherapy in relation to cytokine release, the blood-brain barrier, and cognitive impairment. *Oncol Nurs Forum* 2008; **35**: 916–920.
9 Mekhail TM, Markman M. Paclitaxel in cancer therapy. *Expert Opin Pharmacother* 2002; **3**: 755–766.
10 Alloatti G, Penna C, Gallo MP, Levi RC, Bombardelli E, Appendino G. Differential effects of paclitaxel and derivatives on guinea pig isolated heart and papillary muscle. *J Pharmacol Exp Ther* 1998; **284**: 561–567.
11 Ziske CG, Schottker B, Gorschluter M, Mey U, Kleinschmidt R, Schlegel U *et al.* Acute transient encephalopathy after paclitaxel infusion: report of three cases. *Ann Oncol* 2002; **13**: 629–631.
12 Walz R, Muxfeldt Bianchin M, Kliemann F. Transient encephalopathy after Taxol infusion. *Neurology* 1997; **49**: 1188–1189.
13 Nieto Y, Cagnoni PJ, Bearman SI, Shpall EJ, Matthes S, DeBoom T *et al.* Acute encephalopathy: a new toxicity associated with high-dose paclitaxel. *Clin Cancer Res* 1999; **5**: 501–506.
14 Wefel JS, Saleeba AK, Buzdar AU, Meyers CA. Acute and late onset cognitive dysfunction associated with chemotherapy in women with breast cancer. *Cancer* 2010; **116**: 3348–3356.
15 Smith AE, Slivicki RA, Hohmann AG, Crystal JD. The chemotherapeutic agent paclitaxel selectively impairs learning while sparing source memory and spatial memory. *Behav Brain Res* 2017; **320**: 48–57.
16 Fardell JE, Vardy J, Johnston IN. The short and long term effects of docetaxel chemotherapy on rodent object recognition and spatial reference memory. *Life Sci* 2013; **93**: 596–604.
17 Callaghan CK, O'Mara SM. Long-term cognitive dysfunction in the rat following docetaxel treatment is ameliorated by the phosphodiesterase-4 inhibitor, rolipram. *Behav Brain Res* 2015; **290**: 84–89.
18 Boyette-Davis JA, Fuchs PN. Differential effects of paclitaxel treatment on cognitive functioning and mechanical sensitivity. *Neurosci Lett* 2009; **453**: 170–174.
19 Katsumata N, Yasuda M, Takahashi F, Isonishi S, Jobo T, Aoki D *et al.* Dose-dense paclitaxel once a week in combination with carboplatin every 3 weeks for advanced ovarian cancer: a phase 3, open-label, randomised controlled trial. *Lancet* 2009; **374**: 1331–1338.
20 Kronenberg G, Gertz K, Baldinger T, Kirste I, Eckart S, Yildirim F *et al.* Impact of actin filament stabilization on adult hippocampal and olfactory bulb neurogenesis. *J Neurosci* 2010; **30**: 3419–3431.
21 Capela JP, Ruscher K, Lautenschlager M, Freyer D, Dirnagl U, Gaio AR *et al.* Ecstasy-induced cell death in cortical neuronal cultures is serotonin 2 A-receptor-dependent and potentiated under hyperthermia. *Neuroscience* 2006; **139**: 1069–1081.
22 Chambers SM, Fasano CA, Papapetrou EP, Tomishima M, Sadelain M, Studer L. Highly efficient neural conversion of human ES and iPS cells by dual inhibition of SMAD signaling. *Nat Biotechnol* 2009; **27**: 275–280.
23 Boehmerle W, Muenzfeld H, Springer A, Huehnchen P, Endres M. Specific targeting of neurotoxic side effects and pharmacological profile of the novel cancer stem cell drug salinomycin in mice. *J Mol Med* 2014; **92**: 889–900.
24 Boehmerle W, Endres M. Salinomycin induces calpain and cytochrome c-mediated neuronal cell death. *Cell Death Dis* 2011; **2**: e168.
25 Boehmerle W, Zhang K, Sivula M, Heidrich FM, Lee Y, Jordt SE *et al.* Chronic exposure to paclitaxel diminishes phosphoinositide signaling by calpain-mediated neuronal calcium sensor-1 degradation. *Proc Natl Acad Sci USA* 2007; **104**: 11103–11108.
26 Huehnchen P, Boehmerle W, Endres M. Assessment of paclitaxel induced sensory polyneuropathy with "Catwalk" automated gait analysis in mice. *PLoS ONE* 2013; **8**: e76772.
27 Atas A, Agca O, Sarac S, Poyraz A, Akyol MU. Investigation of ototoxic effects of Taxol on a mice model. *Int J Pediatr Otorhinolaryngol* 2006; **70**: 779–784.
28 Suresh K. An overview of randomization techniques: An unbiased assessment of outcome in clinical research. *J Hum Reprod Sci* 2011; **4**: 8–11.

29 Ferrando-Climent L, Rodriguez-Mozaz S, Barcelo D. Development of a UPLC-MS/MS method for the determination of ten anticancer drugs in hospital and urban wastewaters, and its application for the screening of human metabolites assisted by information-dependent acquisition tool (IDA) in sewage samples. *Analyt Bioanalyt Chem* 2013; **405**: 5937–5952.
30 Kronenberg G, Harms C, Sobol RW, Cardozo-Pelaez F, Linhart H, Winter B *et al.* Folate deficiency induces neurodegeneration and brain dysfunction in mice lacking uracil DNA glycosylase. *J Neurosci* 2008; **28**: 7219–7230.
31 Boehmerle W, Huehnchen P, Peruzzaro S, Balkaya M, Endres M. Electrophysiological, behavioral and histological characterization of paclitaxel, cisplatin, vincristine and bortezomib-induced neuropathy in C57Bl/6 mice. *Sci Rep* 2014; **4**: 6370.
32 Kronenberg G, Balkaya M, Prinz V, Gertz K, Ji S, Kirste I *et al.* Exofocal dopaminergic degeneration as antidepressant target in mouse model of poststroke depression. *Biol Psychiatry* 2012; **72**: 273–281.
33 Kilkenny C, Browne WJ, Cuthill IC, Emerson M, Altman DG. Improving bioscience research reporting: the ARRIVE guidelines for reporting animal research. *PLoS Biol* 2010; **8**: e1000412.
34 Dardis C. Peirce's criterion for the rejection of non-normal outliers; defining the range of applicability. *J Stat Softw* 2004; **10**: 1–8.
35 Ross SM. Peirce's criterion for the elimination of suspect experimental data. *J Eng Technol* 2003; **20**: 38–41.
36 Fellner S, Bauer B, Miller DS, Schaffrik M, Fankhanel M, Spruss T *et al.* Transport of paclitaxel (Taxol) across the blood-brain barrier *in vitro* and *in vivo*. *J Clin Invest* 2002; **110**: 1309–1318.
37 Eiseman JL, Eddington ND, Leslie J, MacAuley C, Sentz DL, Zuhowski M *et al.* Plasma pharmacokinetics and tissue distribution of paclitaxel in CD2F1 mice. *Cancer Chemother Pharmacol* 1994; **34**: 465–471.
38 Morris RG, Garrud P, Rawlins JN, O'Keefe J. Place navigation impaired in rats with hippocampal lesions. *Nature* 1982; **297**: 681–683.
39 Maei HR, Zaslavsky K, Teixeira CM, Frankland PW. What is the most sensitive measure of water maze probe test performance? *Front Integr Neurosci* 2009; **3**: 4.
40 Miller K, Massie MJ. Depression and anxiety. *Cancer J* 2006; **12**: 388–397.
41 Garthe A, Behr J, Kempermann G. Adult-generated hippocampal neurons allow the flexible use of spatially precise learning strategies. *PLoS ONE* 2009; **4**: e5464.
42 Zhang CL, Zou Y, He W, Gage FH, Evans RM. A role for adult TLX-positive neural stem cells in learning and behaviour. *Nature* 2008; **451**: 1004–1007.
43 Temple S. Defining neural stem cells and their role in normal development of the nervous system. In: Rao MS (ed). *Neural Development and Stem Cells*. Humana Press: Totowa, NJ, USA, 2006, pp 1–28.
44 Boehmerle W, Splittgerber U, Lazarus MB, McKenzie KM, Johnston DG, Austin DJ *et al.* Paclitaxel induces calcium oscillations via an inositol 1,4,5-trisphosphate receptor and neuronal calcium sensor 1-dependent mechanism. *Proc Natl Acad Sci USA* 2006; **103**: 18356–18361.
45 Schlecker C, Boehmerle W, Jeromin A, DeGray B, Varshney A, Sharma Y *et al.* Neuronal calcium sensor-1 enhancement of InsP3 receptor activity is inhibited by therapeutic levels of lithium. *J Clin Invest* 2006; **116**: 1668–1674.
46 Mo M, Erdelyi I, Szigeti-Buck K, Benbow JH, Ehrlich BE. Prevention of paclitaxel-induced peripheral neuropathy by lithium pretreatment. *FASEB J* 2012; **26**: 4696–4709.
47 Gratzner HG. Monoclonal antibody to 5-bromo- and 5-iododeoxyuridine: a new reagent for detection of DNA replication. *Science* 1982; **218**: 474–475.
48 Kempermann G, Kuhn HG, Gage FH. More hippocampal neurons in adult mice living in an enriched environment. *Nature* 1997; **386**: 493–495.
49 Vardy J, Tannock I. Cognitive function after chemotherapy in adults with solid tumours. *Crit Rev Oncol/Hematol* 2007; **63**: 183–202.
50 Ahles TA, Root JC, Ryan EL. Cancer- and cancer treatment-associated cognitive change: an update on the state of the science. *J Clin Oncol* 2012; **30**: 3675–3686.
51 Taillibert S, Voillery D, Bernard-Marty C. Chemobrain: is systemic chemotherapy neurotoxic? *Curr Opin Oncol* 2007; **19**: 623–627.
52 Wang XM, Walitt B, Saligan L, Tiwari AF, Cheung CW, Zhang ZJ. Chemobrain: a critical review and causal hypothesis of link between cytokines and epigenetic reprogramming associated with chemotherapy. *Cytokine* 2015; **72**: 86–96.
53 Weiss B. Chemobrain: a translational challenge for neurotoxicology. *Neurotoxicology* 2008; **29**: 891–898.
54 Seigers R, Fardell JE. Neurobiological basis of chemotherapy-induced cognitive impairment: a review of rodent research. *Neurosci Biobehav Rev* 2011; **35**: 729–741.
55 Scherling CS, Smith A. Opening up the window into "chemobrain": a neuroimaging review. *Sensors* 2013; **13**: 3169–3203.
56 Dubois M, Lapinte N, Villier V, Lecointre C, Roy V, Tonon MC *et al.* Chemotherapy-induced long-term alteration of executive functions and hippocampal cell proliferation: role of glucose as adjuvant. *Neuropharmacology* 2014; **79**: 234–248.
57 Georgiadis MS, Russell EK, Gazdar AF, Johnson BE. Paclitaxel cytotoxicity against human lung cancer cell lines increases with prolonged exposure durations. *Clin Cancer Res* 1997; **3**: 449–454.
58 Liebmann JE, Cook JA, Lipschultz C, Teague D, Fisher J, Mitchell JB. Cytotoxic studies of paclitaxel (Taxol) in human tumour cell lines. *Br J Cancer* 1993; **68**: 1104–1109.
59 Schiff PB, Fant J, Horwitz SB. Promotion of microtubule assembly *in vitro* by taxol. *Nature* 1979; **277**: 665–667.
60 Zhang K, Heidrich FM, DeGray B, Boehmerle W, Ehrlich BE. Paclitaxel accelerates spontaneous calcium oscillations in cardiomyocytes by interacting with NCS-1 and the InsP3R. *J Mol Cell Cardiol* 2010; **49**: 829–835.
61 Vanden Berghe T, Linkermann A, Jouan-Lanhouet S, Walczak H, Vandenabeele P. Regulated necrosis: the expanding network of non-apoptotic cell death pathways. *Nat Rev Mol Cell Biol* 2014; **15**: 135–147.
62 Baudry M, Bi X. Calpain-1 and calpain-2: the Yin and Yang of synaptic plasticity and neurodegeneration. *Trends Neurosci* 2016; **39**: 235–245.
63 Trinchese F, Fa M, Liu S, Zhang H, Hidalgo A, Schmidt SD *et al.* Inhibition of calpains improves memory and synaptic transmission in a mouse model of Alzheimer disease. *J Clin Invest* 2008; **118**: 2796–2807.
64 Kidd JF, Pilkington MF, Schell MJ, Fogarty KE, Skepper JN, Taylor CW *et al.* Paclitaxel affects cytosolic calcium signals by opening the mitochondrial permeability transition pore. *J Biol Chem* 2002; **277**: 6504–6510.
65 Benbow JH, Mann T, Keeler C, Fan C, Hodsdon ME, Lolis E *et al.* Inhibition of paclitaxel-induced decreases in calcium signaling. *J Biol Chem* 2012; **287**: 37907–37916.
66 Gao M, Yan X, Weng HR. Inhibition of glycogen synthase kinase 3beta activity with lithium prevents and attenuates paclitaxel-induced neuropathic pain. *Neuroscience* 2013; **254**: 301–311.
67 Penson RT, Kronish K, Duan Z, Feller AJ, Stark P, Cook SE *et al.* Cytokines IL-1beta, IL-2, IL-6, IL-8, MCP-1, GM-CSF and TNFalpha in patients with epithelial ovarian cancer and their relationship to treatment with paclitaxel. *Int J Gynecol Cancer* 2000; **10**: 33–41.
68 Carletti F, Sardo P, Gambino G, Liu XA, Ferraro G, Rizzo V. Hippocampal hyperexcitability is modulated by microtubule-active agent: evidence from *in vivo* and *in vitro* epilepsy models in the rat. *Front Cell Neurosci* 2016; **10**: 29.
69 Chen G, Rajkowska G, Du F, Seraji-Bozorgzad N, Manji HK. Enhancement of hippocampal neurogenesis by lithium. *J Neurochem* 2000; **75**: 1729–1734.
70 Kim JS, Chang MY, Yu IT, Kim JH, Lee SH, Lee YS *et al.* Lithium selectively increases neuronal differentiation of hippocampal neural progenitor cells both *in vitro* and *in vivo*. *J Neurochem* 2004; **89**: 324–336.
71 Senatorov VV, Ren M, Kanai H, Wei H, Chuang DM. Short-term lithium treatment promotes neuronal survival and proliferation in rat striatum infused with quinolinic acid, an excitotoxic model of Huntington's disease. *Mol Psychiatry* 2004; **9**: 371–385.
72 Li H, Li Q, Du X, Sun Y, Wang X, Kroemer G *et al.* Lithium-mediated long-term neuroprotection in neonatal rat hypoxia-ischemia is associated with antiinflammatory effects and enhanced proliferation and survival of neural stem/progenitor cells. *J Cereb Blood Flow Metab* 2011; **31**: 2106–2115.
73 Wood AJ, Goodwin GM, De Souza R, Green AR. The pharmacokinetic profile of lithium in rat and mouse; an important factor in psychopharmacological investigation of the drug. *Neuropharmacology* 1986; **25**: 1285–1288.
74 Oruch R, Elderbi MA, Khattab HA, Pryme IF, Lund A. Lithium: a review of pharmacology, clinical uses, and toxicity. *Eur J Pharmacol* 2014; **740**: 464–473.

Supplementary Information accompanies the paper on the *Translational Psychiatry* website (http://www.nature.com/tp)